

THE UNIVERSITY OF CHICAGO

EVIDENCE FOR ANTARCTIC ALTERATION
OF MARTIAN METEORITE ALH84001

A SENIOR THESIS SUBMITTED
IN PARTIAL FULFILLMENT OF
THE REQUIREMENTS FOR DEPARTMENTAL HONORS
WITH THE DEGREE OF
BACHELOR OF SCIENCE IN GEOPHYSICAL SCIENCES

THE COLLEGE

BY
ROBERT E. KOPP III

CHICAGO, ILLINOIS

APRIL 2002

Evidence for Antarctic alteration of Martian meteorite

ALH84001

Robert E. Kopp III

11 April 2002

Abstract

The magnetites and sulfides located in the rims of carbonate globules in the Martian meteorite ALH84001 have been claimed as evidence of past life on Mars. The globules' chemical zonation patterns suggest that the rims may be a product of weathering processes. A kinetic model was used to examine the possibility that these rims formed through the dissolution and reprecipitation of a primary Martian carbonate while the meteorite was exposed at the surface in Antarctica. The results suggest that the formation of the rims under such conditions would take less than fifty years, and that sufficient time was therefore available for the rims to form in Antarctica. If this model is correct, then any biogenic features in the rims are most likely the products of terrestrial, rather than Martian, life.

1 Introduction

ALH84001 is a basaltic Martian meteorite, recovered from Allan Hills, Antarctica, in 1984, and later linked by oxygen isotope data to the Martian meteorites of the SNC clan (Mittlefehldt, 1994; Clayton, 1993). Composed primarily of orthopyroxene, the meteorite contains a number of trace phases, including olivine, chromite, maskelynite, pyrite, and Mg-Fe-Ca-Mn carbonate.

Carbonate generally occurs in zoned globules, discoid grains of magnesite from $\sim 50 \mu\text{m}$ to $\sim 200 \mu\text{m}$ in diameter and $\sim 10 \mu\text{m}$ to $\sim 30 \mu\text{m}$ thick located on fracture surfaces in the meteorite (McKay et al., 1996; Romanek et al., 1995; Mittlefehldt, 1997). These globules have high-Ca, low-Fe cores and are surrounded by rims composed of thin alternating Fe-rich and Mg-rich bands. The Fe-rich bands contain abundant magnetite grains, including some which resemble those produced by magnetotactic bacteria (Thomas-Keprta et al., 2000), as well as trace amounts of sulfide minerals including pyrrhotite and greigite (McKay et al., 1996).

McKay et al. (1996) set out four lines of argument suggesting that this meteorite contained evidence of past life on Mars: (1) the presence of organic carbon in the form of polycyclic aromatic hydrocarbons (PAHs) within the meteorite, (2) the presence of elongate ovoids resembling terrestrial bacterial microfossils associated with carbonate phases, (3) oxygen isotope data suggesting carbonate formation at temperatures between 0° and 80°C , temperatures compatible with the existence of life, and (4) the presence of magnetites and sulfides, which can form as a product of biological activity on Earth, in association with the carbonates. Other researchers, however, have argued that the PAHs could be a product of a combination of terrestrial contamination, formation during impact heating, and delivery to the Martian surface by meteoritic or cometary debris (Becker et al., 1997, 1999; Jull et al., 1998). Research by Bradley et al. (1997) concluded that the alleged microfossils were abiogenic structures; Grady et al. (1997) wondered whether belief in such microfossils was “a question of faith.”

Of McKay et al.'s four original arguments, the most resilient have been their arguments about the formation temperature of the carbonate globules and the presence of magnetite and sulfides. A number of alternative hypotheses about the origin of the carbonate globules and their rims have been proposed. One model by Harvey and McSween (1996) suggested the globules formed from a high-temperature interaction between CO_2 -rich fluids and orthopyroxene, with rapid cooling preserving the disequilibrium exhibited in the zonation of the rims. A different model by the same pair (McSween and Harvey, 1998) proposed that the globules formed at low temperature from an evaporating brine infiltrating impact crater fractures, with zonation reflecting sudden changes in the

precipitation environment. Warren (1998) suggested a similar process, with the globules forming as flood evaporites, possibly in a playa lake-type environment. Scott (1999) proposed that the carbonates originally formed as evaporites, and were later subject to impact shock heated and partial vaporization, during which the magnetites formed. Golden et al. (2000, 2001) proposed a mildly hydrothermal origin at temperatures around 150°C, with zonation resulting from a change in solution composition due to the precipitation of kinetically-favored carbonates, and magnetites forming by siderite decomposition during a brief heating to 470°C.

While the compositions of the globules are compatible with a Martian origin, it is possible that the rims are of a later origin than the central crystals. In particular, these rims may have formed through the dissolution and reprecipitation of carbonate while ALH84001 was exposed to surface conditions in Antarctica. This might have happened either immediately after the meteorite's landing ~13,000 y.a. (Jull et al., 1995) and before its burial in the Antarctic ice, or in modern times, after its re-exposure to the surface. If this were the case, Occam's Razor would suggest that the apparently biogenic features associated with the rims are also of terrestrial origin. This paper describes petrographic evidence for the formation of the rims by weathering processes and a kinetic model used to determine the conditions required for such processes to produce the rims.

2 Methodology

2.1 Petrography and Chemical Analysis

A JEOL JSM5800LV scanning electron microscope equipped with an Oxford Link ISIS-300 X-ray analysis system was used to examine carbonate globules on the fracture surface of ALH84001,265. The specimen was coated with carbon to improve conductivity, and measurements were made in high-vacuum mode ($P < 10^{-4}$ torr) to reduce beam scattering. To calculate molecular composition based on an elemental analysis with the X-ray system, the following procedure was used:

1. All Si was assumed to reside in orthopyroxene. The mean composition for orthopyroxene measured by Mittlefehldt (1994), $Wo_{3.3}En_{69.4}Fs_{27.3}$, was used.

Reaction	log K (25°C)	Ref.
$>\text{CO}_3\text{H}^0 = >\text{CO}_3^- + \text{H}^+$	-4.65	a
$>\text{CO}_3\text{H}^0 + \text{Mg}^{+2} = >\text{CO}_3\text{Mg}^+ + \text{H}^+$	-2.20	a
$>\text{MgOH}^0 = >\text{MgO}^- + \text{H}^+$	-12	a
$>\text{MgOH}^0 + \text{H}^+ = >\text{MgOH}_2^+$	10.60	a
$>\text{MgOH}^0 + \text{CO}_3^{-2} + \text{H}^+ = >\text{MgCO}_3^- + \text{H}_2\text{O}$	14.40	a
$>\text{MgOH}^0 + \text{CO}_3^{-2} + 2\text{H}^+ = >\text{MgHCO}_3^0 + \text{H}_2\text{O}$	22.40	a
$\text{MgCO}_3(\text{s}) = \text{Mg}^{+2} + \text{CO}_3^{-2}$	-8.029	b
$\text{FeCO}_3(\text{s}) = \text{Fe}^{+2} + \text{CO}_3^{-2}$	-10.55	b
$\text{Mg}^{+2} + \text{H}_2\text{O} = \text{MgOH}^+ + \text{H}^+$	-11.79	b
$\text{Mg}^{+2} + \text{CO}_3^{-2} = \text{MgCO}_3(\text{aq})$	2.98	b
$\text{Mg}^{+2} + \text{H}^+ + \text{CO}_3^{-2} = \text{MgHCO}_3^+$	11.40	b
$\text{Fe}^{+3} + \text{e}^- = \text{Fe}^{+2}$	13.032	b
$\text{Fe}^{+2} + \text{H}_2\text{O} = \text{FeOH}^+ + \text{H}^+$	-9.5	b
$\text{Fe}^{+2} + 3\text{H}_2\text{O} = \text{Fe}(\text{OH})_3^- + 3\text{H}^+$	-31	b
$\text{Fe}^{+2} + 2\text{H}_2\text{O} = \text{Fe}(\text{OH})_2 + 2\text{H}^+$	-20.57	b
$\text{Fe}^{+3} + \text{H}_2\text{O} = \text{FeOH}^{+2} + \text{H}^+$	-2.19	b
$\text{Fe}^{+3} + 2\text{H}_2\text{O} = \text{Fe}(\text{OH})_2^+ + 2\text{H}^+$	-5.67	b
$\text{Fe}^{+3} + 3\text{H}_2\text{O} = \text{Fe}(\text{OH})_3 + 3\text{H}^+$	-13.6	b
$\text{Fe}^{+3} + 4\text{H}_2\text{O} = \text{Fe}(\text{OH})_4^- + 4\text{H}^+$	-21.6	b
$2\text{Fe}^{+3} + 2\text{H}_2\text{O} = \text{Fe}_2(\text{OH})_2^{+4} + 2\text{H}^+$	-2.95	b
$3\text{Fe}^{+3} + 4\text{H}_2\text{O} = \text{Fe}_3(\text{OH})_4^{+5} + 4\text{H}^+$	-6.3	b
$\text{CO}_2(\text{g}) + \text{H}_2\text{O} = \text{CO}_3^{-2} + 2\text{H}^+$	-18.16	b
$\text{CO}_3^{-2} + \text{H}^+ = \text{HCO}_3^-$	10.33	b
$\text{CO}_3^{-2} + 2\text{H}^+ = \text{CO}_2(\text{aq}) + \text{H}_2\text{O}$	16.681	b

Sources: a–Pokrovsky et al. (1999); b–MINTEQ database.

Table 1: Internal stability constants and solubility constants used in this model.

2. All Cr was assumed to reside in chromite, FeCr_2O_4 .
3. All S was assumed to reside in an iron sulfide with the composition FeS .
4. All Mn was assumed to reside in MnCO_3 .
5. The remaining Mg was assumed to reside in MgCO_3 .
6. The remaining Ca was assumed to reside in CaCO_3 .
7. The remaining Fe was assumed to reside in either ferrous carbonate or magnetite, and was allocated to the compound phase “ $\text{Fe}(\text{CO}_3, \text{O}_{1.33})$ ”.

2.2 Kinetic model

Magnesite surface speciation and magnesite and siderite dissolution rates were modeled using PHREEQC, a program publicly available from the USGS (Parkhurst and Appelo, 1999). For equilibrium calculations, PHREEQC uses a modified version of the Newton-Raphson iterative method to simultaneously solve mass balance, activity, and thermodynamic equilibrium equations. For kinetic calculations, PHREEQC employs an individually defined time-stepped algorithm for the rate of each reaction.

The empirically determined 25°C stability constants for magnesite surface species from Pokrovsky et al. (1999) (see Table 1), the magnesite dissolution rate formula from Pokrovsky and Schott (1999), and the siderite dissolution rate formula from Dresel (1989) were used in the calculations. The magnesite dissolution rate formula is a function of the concentration of the surface species $>CO_3H^0$ and $>MgOH_2^+$:

$$R(\text{mol m}^{-2} \text{s}^{-1}) = [10^{11.198} \cdot \{>CO_3H^0\}^{3.97} + 10^{9.38} \cdot \{>MgOH_2^+\}^{3.94}] \cdot (1 - \exp(-4A/\mathbf{RT})) \quad (1)$$

where $\{> i\}$ represents the concentration in mol m^{-2} of surface species $> i$, \mathbf{R} is the gas constant, T is temperature in Kelvin, and A is the chemical affinity for the reaction, defined as

$$A = -\mathbf{RT} \ln(Q/K_{sp}^0) \quad (2)$$

where Q is the ion activity product and K_{sp}^0 is the magnesite solubility product. A surface species $> xy$ refers to an ion x on the surface of the crystal and a complex y to which it is weakly bonded. Unlike the magnesite dissolution rate formula, the siderite dissolution rate formula is based upon macroscopic parameters, specifically the activities of H^+ , Fe^{2+} , and HCO_3^- :

$$R(\text{mol m}^{-2} \text{s}^{-1}) = 10^{-4.58} (a_{H^+})^{0.75} - 10^{-4.07} (a_{Fe^{2+}} a_{HCO_3^-})^{0.75} \quad (3)$$

where a_j is the activity of aqueous species j .

The surface speciation model employed by PHREEQC is based upon that described by Dzombak and Morel (1990). This model used stability constants that account for non-ideality resulting from Coulombic

interactions by inclusion of an electrostatic term:

$$K_{eff} = K_{int} \cdot \exp(-\Delta z F \Psi_s / RT) \quad (4)$$

where K_{int} is the intrinsic stability constant (given in Table 1), Δz is the change in surface charge produced by a reaction, F is Faraday's constant (96485 C/mol), and Ψ_s is the surface potential. Ψ_s was determined using the method of Borkovec and Westall (1983) to solve the Poisson-Boltzmann equation and determine the composition of a diffuse layer of ions surrounding the surface. This method showed that $\Psi_s \approx 0$, so after the initial runs, models were run under the assumption that $K_{eff} = K_{int}$ and the computationally expensive diffuse layer calculation was omitted.

Because the only rate equations available were for dissolution at 25°C, all trials were run at this temperature. Relative to dissolution occurring near 0°C, this higher temperature should introduce error in two directions. On the one hand, magnesite and siderite become more soluble in colder water, and thus the maximum extent of dissolution should be greater at 0°C than 25°C. Employing 0°C equilibrium constants increased the rate of dissolution while far from equilibrium by a factor of 1.2-1.3. On the other hand, the reaction may proceed somewhat slower at lower temperatures; since no rate data is available at 0°C, the error introduced by this is not quantifiable.

The model considered the cases of carbonate globules immersed in liquid water. Using the appropriate rate equations, the sizes of the globules were tracked in 1-year steps over a period of 200 years. Each trial globule was defined by several different parameters: its composition (either pure magnesite or pure siderite), its size, its surface area-to-volume ratio, the amount of liquid water, and the composition of the atmosphere with which the solution is in equilibrium.

The geometry used in the model was that of a disc, exposed to the solution on its sides, with a fixed height of 10 μm and a variable radius. The surface area-to-volume ratio of such a disc is $\frac{2h}{r}$, where h is the height of the disc and r is the radius of the disc. Values of 50 μm , 75 μm , and 100 μm were used for the initial value of r ; the value of r was recalculated as a function of the amount of carbonate throughout the course of a run. In the case of the siderite trials, the surface area-to-volume ratio was used only in calculating the total loss of carbonate in each step; for the magnesite trials, it was also used in surface speciation calculations to determine the total number of surface sites. (Following Pokrovsky et al. (1999), a density of 18 μmol sites

per m² was assumed.) The value used in the surface speciation calculations was fixed at the beginning of each trial and was not updated during each step; by varying the initial value, this was found to introduce an error of about 25% into the calculations.

The amount of water in which the globule was immersed was varied from 5 μ L to 1 L. Three different atmospheric compositions were used: a terrestrial atmosphere with a pCO₂ of 350 ppm, a modern Martian atmosphere with 8 mbar CO₂, and a hypothetical ancient Martian atmosphere with 1 bar CO₂. The solutions were initially in equilibrium with the atmosphere, but were allowed to depart from this equilibrium as the system evolved.

3 Results

3.1 Petrography and Chemical Analysis

The fracture surface examined (figure 1) contains numerous carbonate globules, many of them overlapping. In backscattered electron mode, carbonate appears slightly darker than the surrounding pyroxene matrix. The alternating Fe-rich and Mg-rich rims around the globules appear bright and dark, respectively. Chromite and sulfides appear as bright regions on the surface. Four carbonate globules or globule clusters were examined in detail.

Globule triplet A (figure 2) consists of three overlapping globules. Due to the high level of topography on this set of globules, it was not possible to conduct a precise X-ray traverse. The element maps, however, qualitatively show several significant features. Each of the three globules in the cluster possesses internal zoning, which is illustrated most clearly in the Ca and Mn maps. The central portions of the three globules are richer in these elements than the more exterior portions. In addition, the outer portion of each globule, just inside the low-Fe rim, is depleted in Ca. The Ca-depleted zones extend fully around each globule and separate them from one another, while the Fe-poor rim and the Fe-rich rim exterior to it extend around all three globules collectively. While the Mg map is overwhelmed by topographic effects, the Fe-poor rim is believed to be Mg rich. S appears to be concentrated in the Fe-rich rim.

Globule D (figures 3, 4, 5, and 6) exhibits less topography than globule triplet A, and it was therefore possible to conduct a traverse. As the maps and the traverse show, the globule possesses a Ca- and Mn-rich interior and Ca-depleted exterior followed by alternating Fe-rich, Mg-rich, and Fe-rich rims. The S-rich regions toward the exterior of this globule coincide precisely with the Fe-rich rims. The Ca-rich phase toward the bottom of the globule is also rich in S and is believed to be a recent contaminant.

Globule pair E (figures 7, 8, 9, and 10) consists of two overlapping carbonate globules. While much of the globules has been eroded to reveal underlying pyroxene, one section of one of the globules, toward the top of the images, is intact and exhibits fairly flat topography. A traverse was conducted on this section. As was the case with the other globules, these globules possess Ca- and Mn-rich interiors, and alternating Fe-rich, Mg-rich, and Fe-rich rims. As in globule triplet A, the two globules are separated by a Ca-poor rings. While S is enriched in the Fe-rich rims, the coincidence of S and Fe enrichment is not as close as in globule D; the Mg-rich rim of this globule also contains a S peak.

Globule cluster F (figure 11), like globule triplet A, possesses too much topography to conduct a precise traverse. The element maps for this cluster reveal that the constituent globules are internally zoned in a fashion similar to the other described globules, although the bottom-right globule seems to possess two high-Ca, high-Mn cores. The globule cluster collectively possesses alternating Fe-rich, Mg-rich, and Fe-rich rims. Unlike the globules that constitute the other clusters described, however, the bottom-left globule of this cluster possesses a Mg-rich rim that surrounds it fully. S appears in the accessory sulfides below the globule, and may also be enriched in the Fe-rich rims.

3.2 Kinetic model

In general, as shown in figure 12, magnesite and siderite dissolve at fairly similar rates, although the two rates can differ by as much as a factor of four. Within the range of values of interest to this study, changes in the surface area-to-volume ratios of the globules had little effect. Although increasing the surface area-to-volume ratio does increase the rate of dissolution, the factor of two

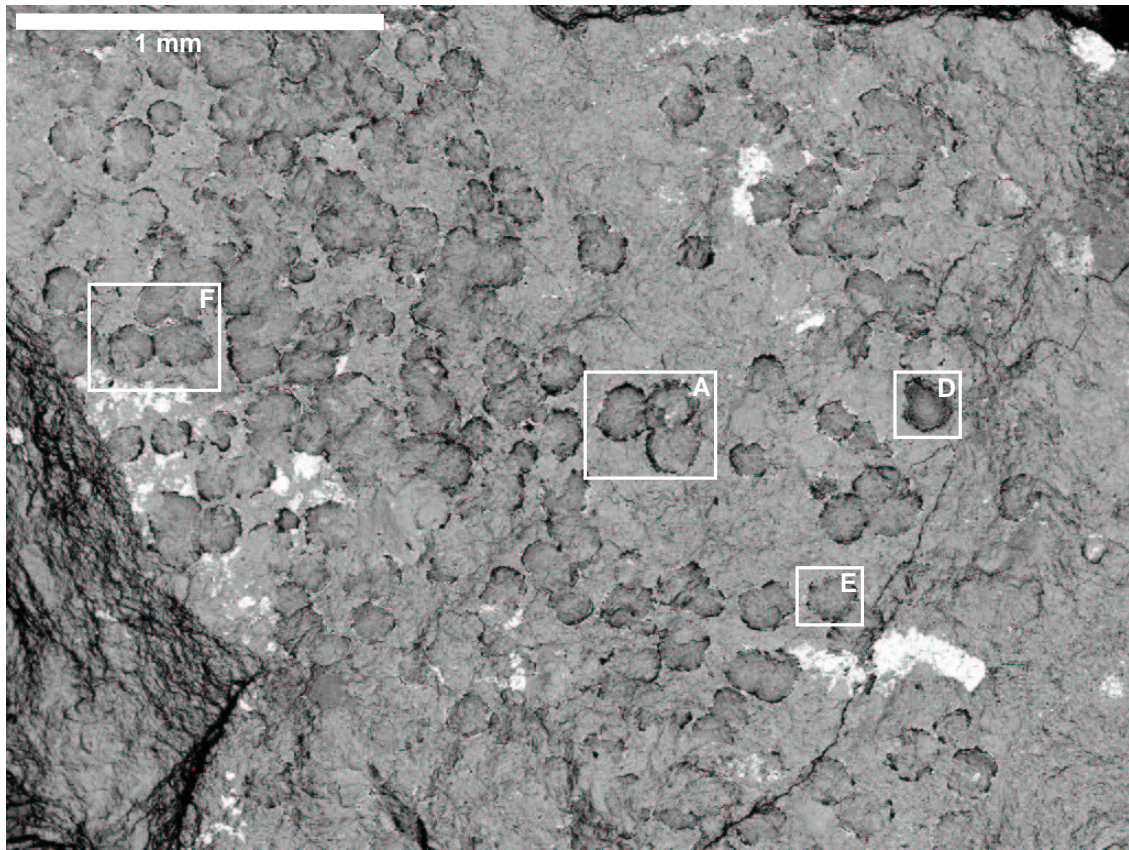


Figure 1: A backscattered electron image of the examined portion of the fracture surface of ALH84001,265. Boxes mark the globules examined in detail.

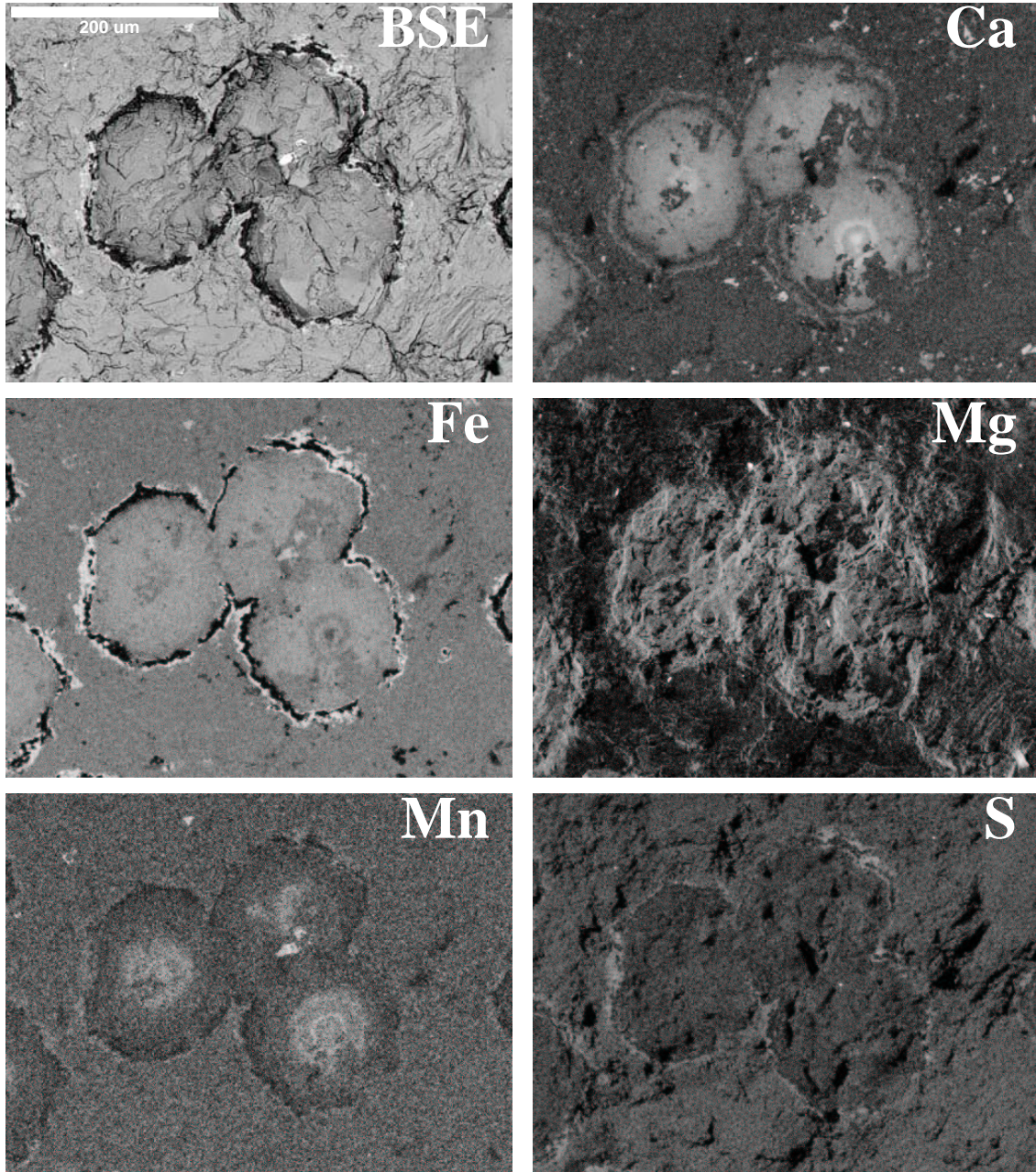


Figure 2: Backscattered electron and element maps of carbonate globule triplet A.

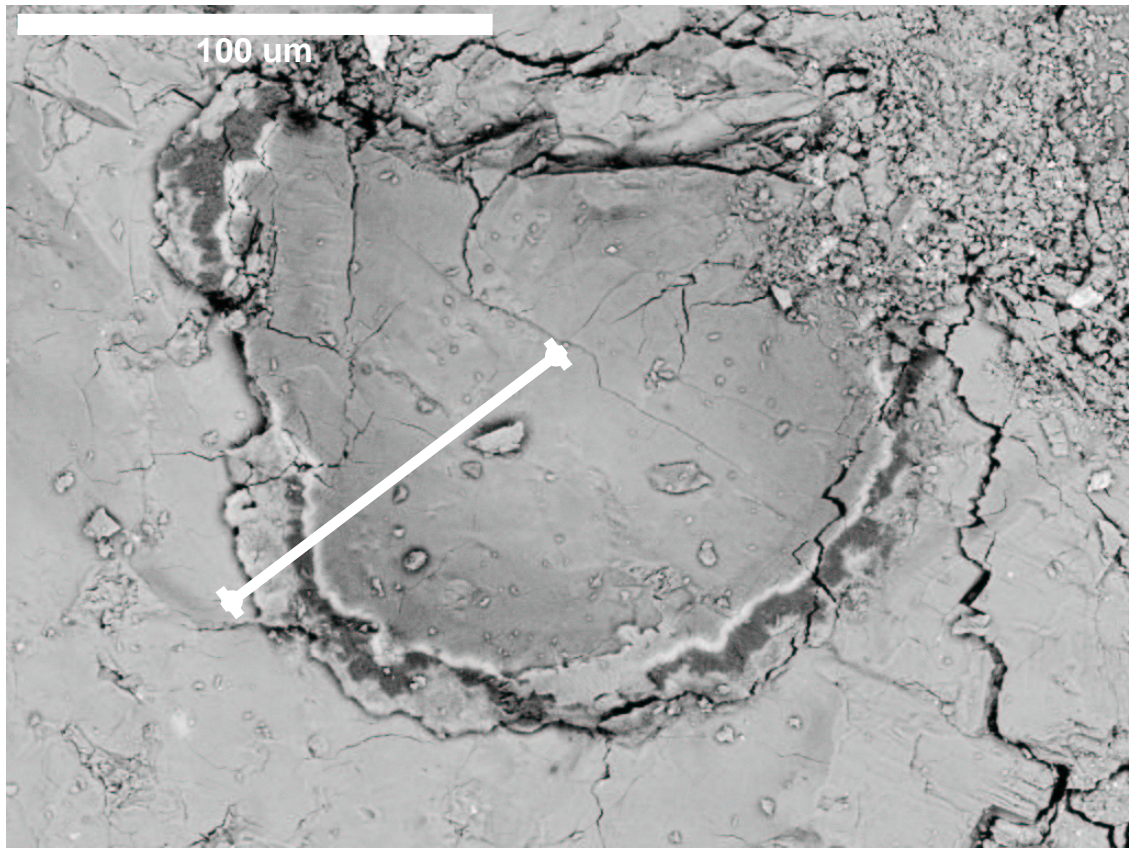


Figure 3: Backscattered electron image of carbonate globule D, with the path of the X-ray traverse show.

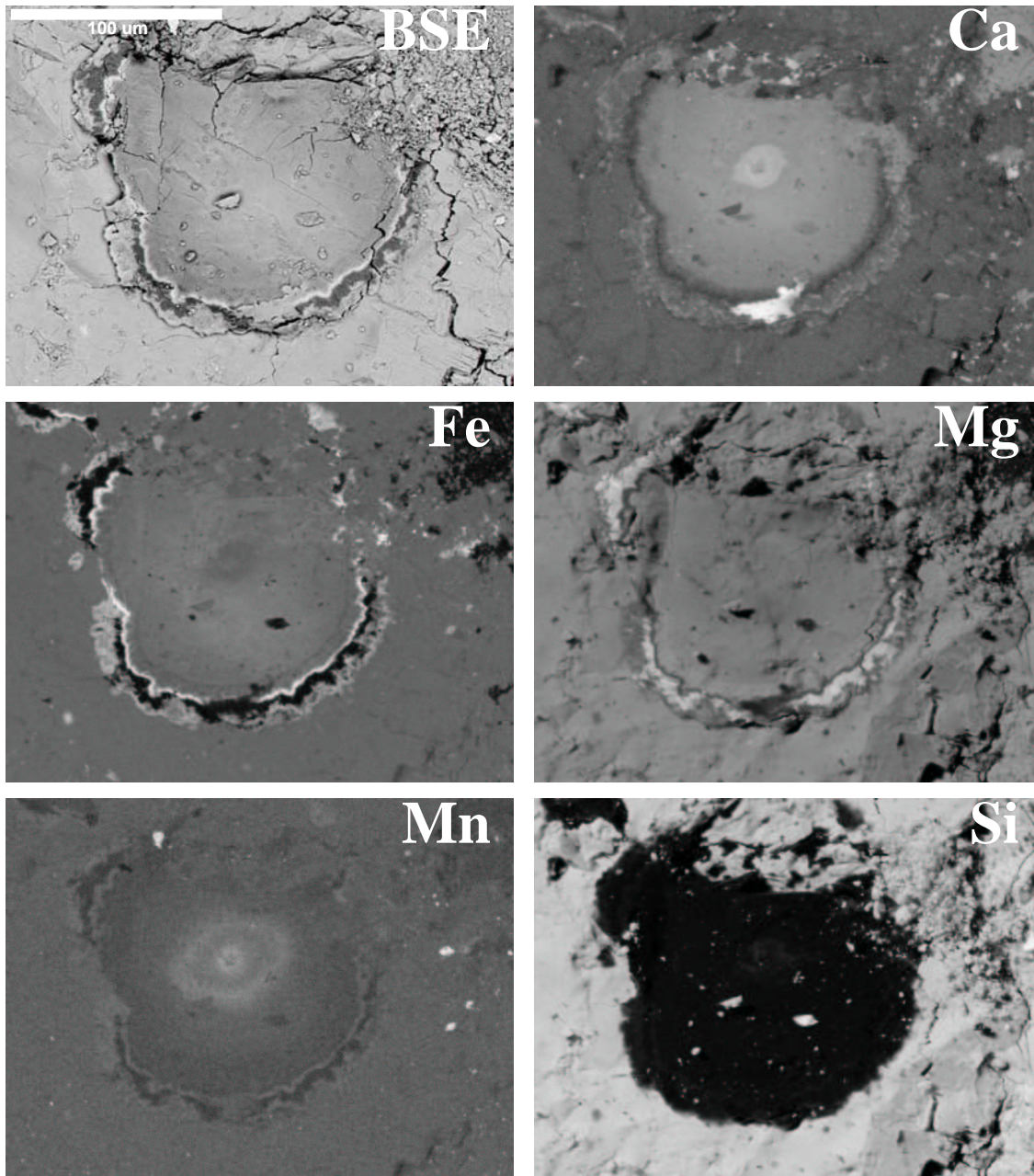


Figure 4: Backscattered electron and element maps of carbonate globule D.

ALH84001 Globule D Traverse

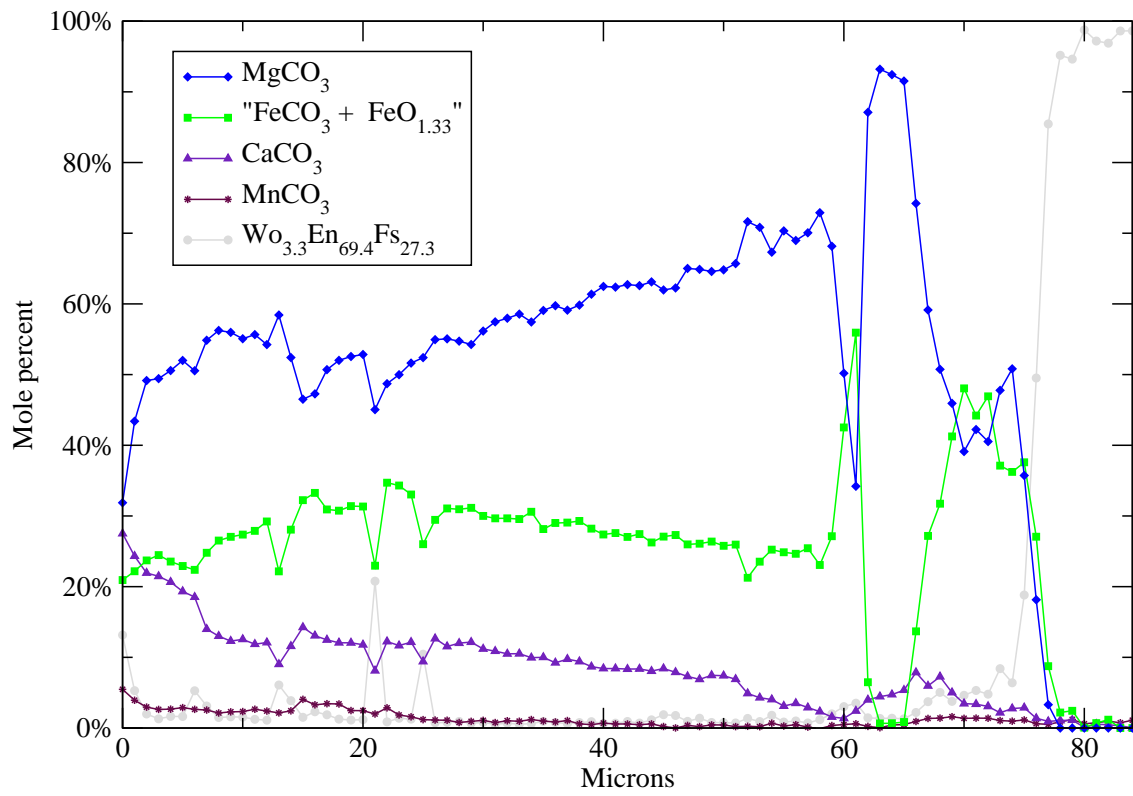


Figure 5: Molecular composition of carbonate globule D from the center of the globule through the rims, based on X-ray analysis data.

ALH84001 Globule D Traverse

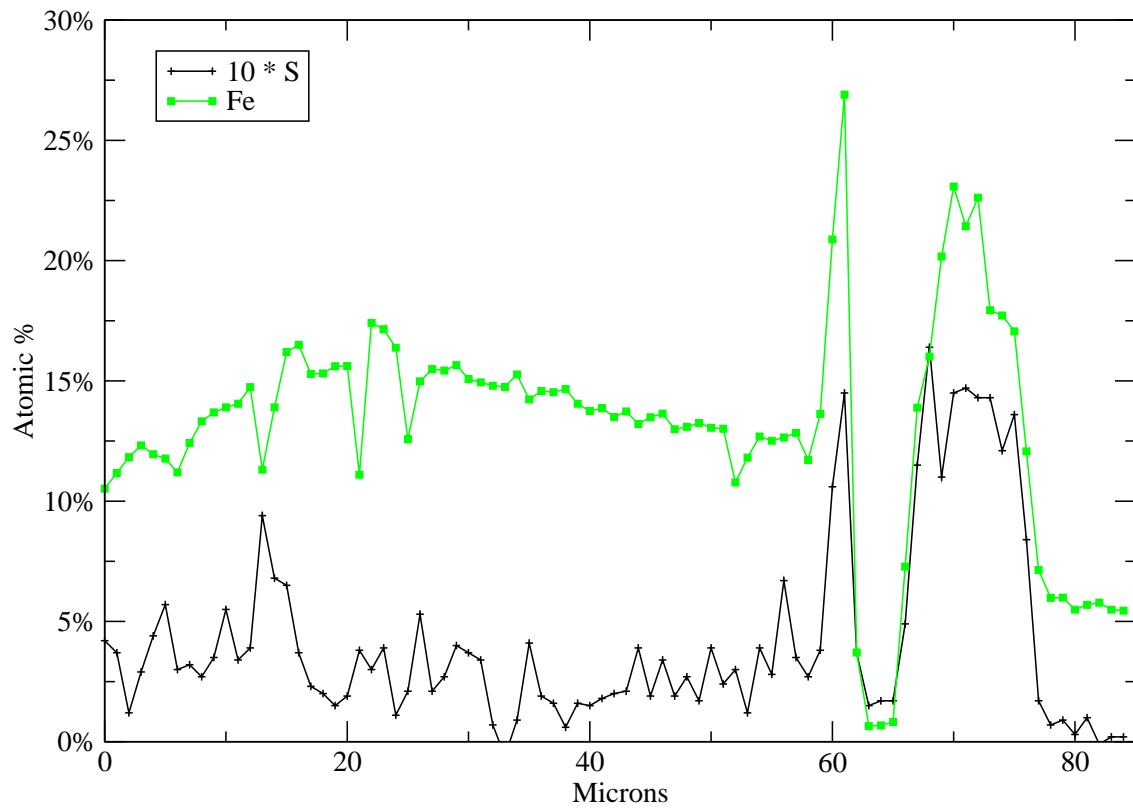


Figure 6: Fe and S composition of carbonate globule D from the center of the globule through the rims, based on X-ray analysis data.

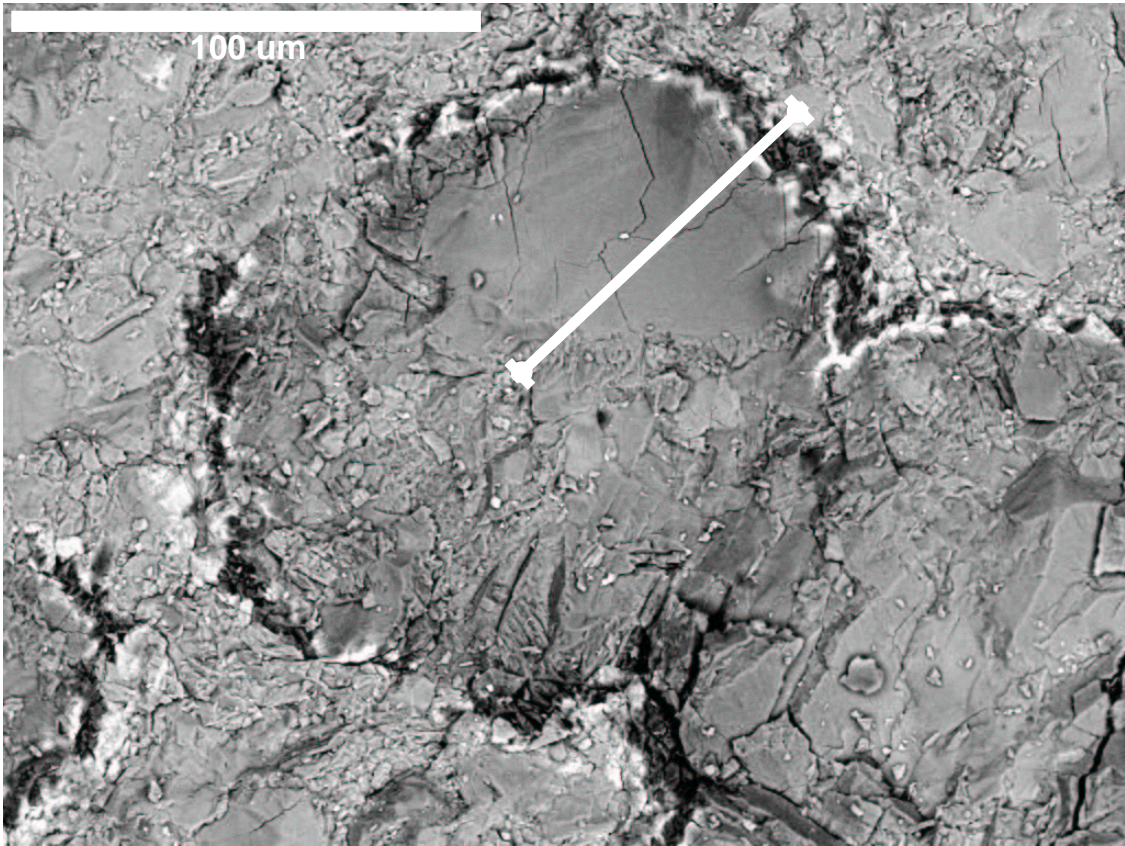


Figure 7: Backscattered electron image of carbonate globule pair E, with the path of the X-ray traverse show.

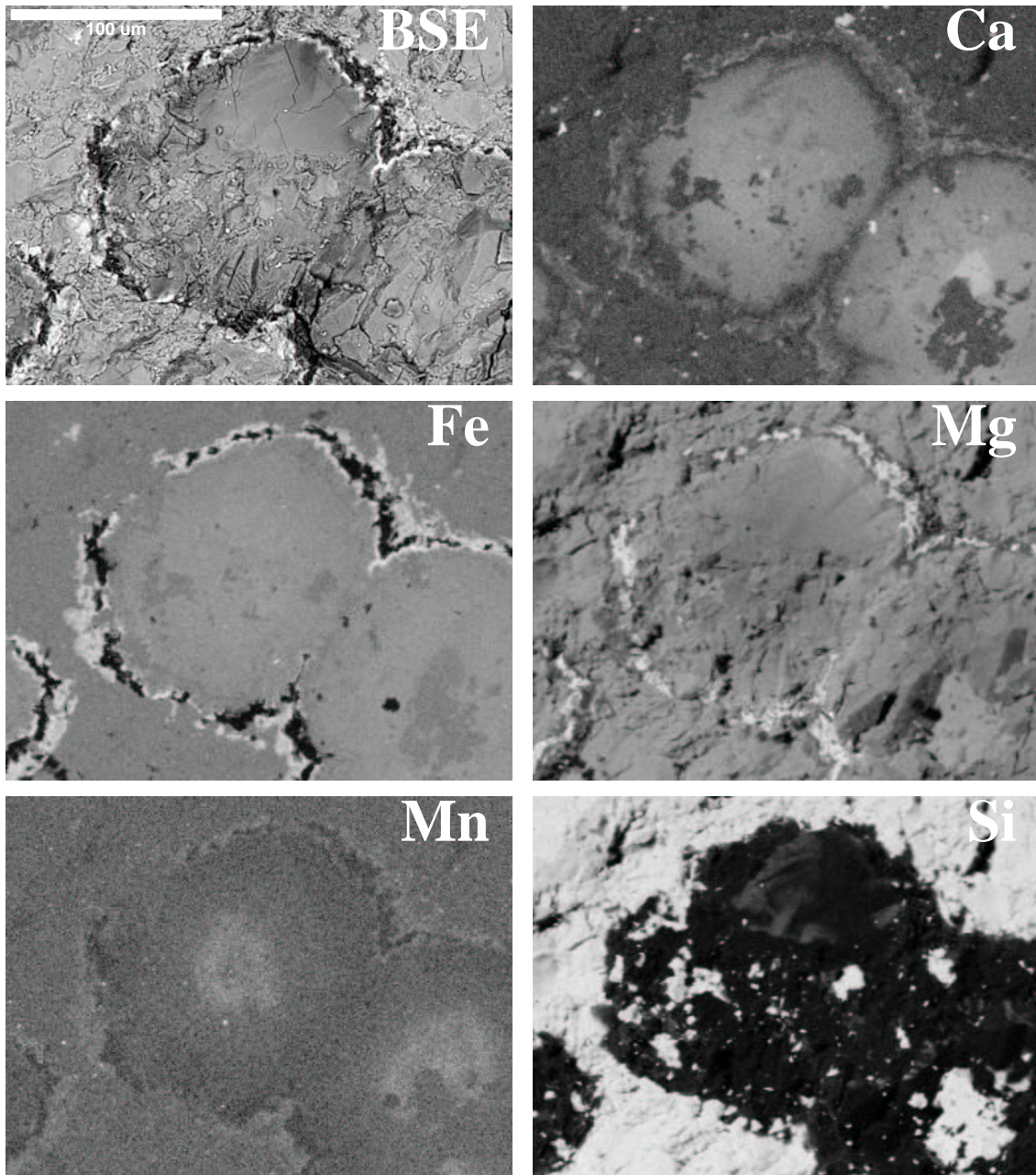


Figure 8: Backscattered electron and element maps of carbonate globule pair E.

ALH84001 Glob E Traverse

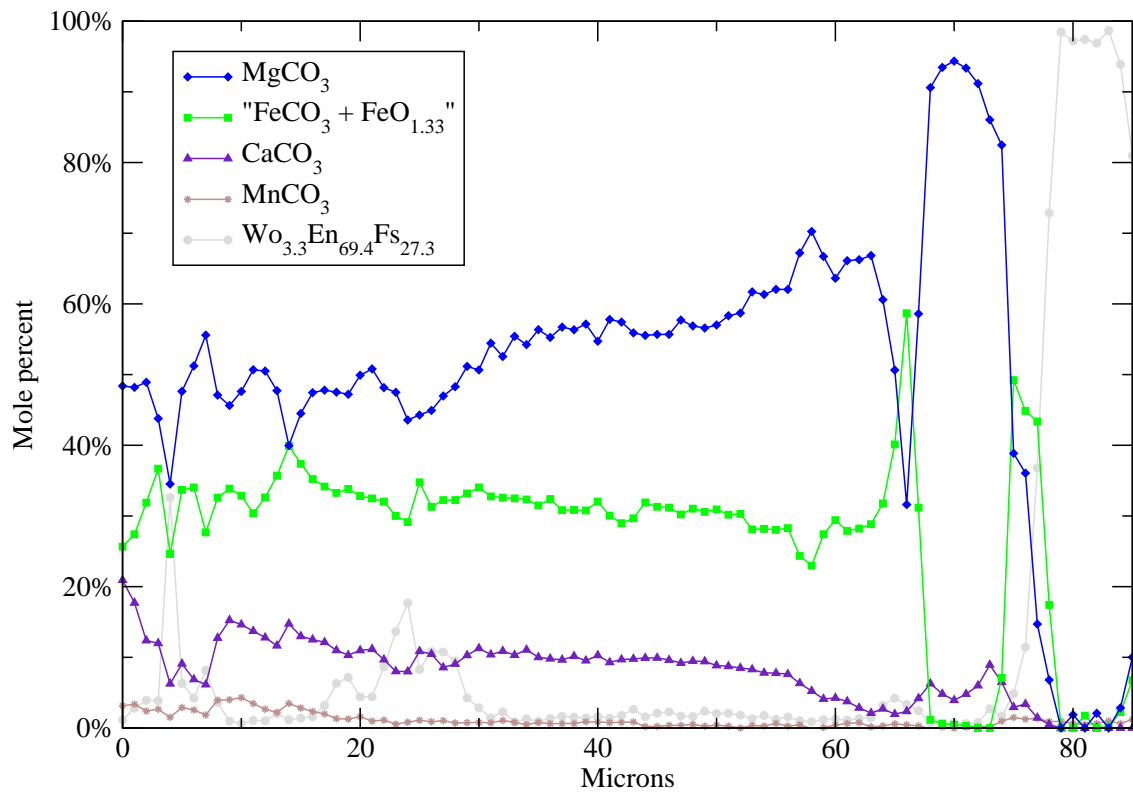


Figure 9: Molecular composition of carbonate globule pair E from the center of the left globule through the rims, based on X-ray analysis data.

ALH84001 Globule E Traverse

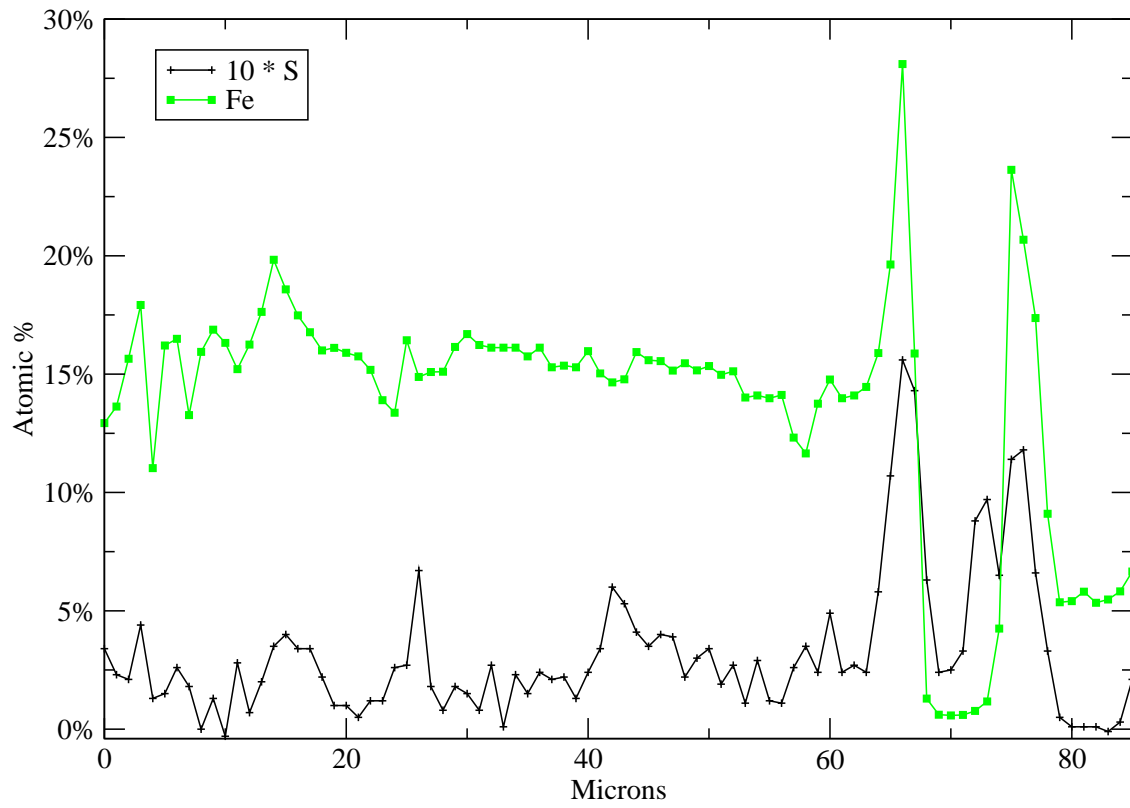


Figure 10: Fe and S composition of carbonate globule pair E from the center of the left globule through the rims, based on X-ray analysis data.

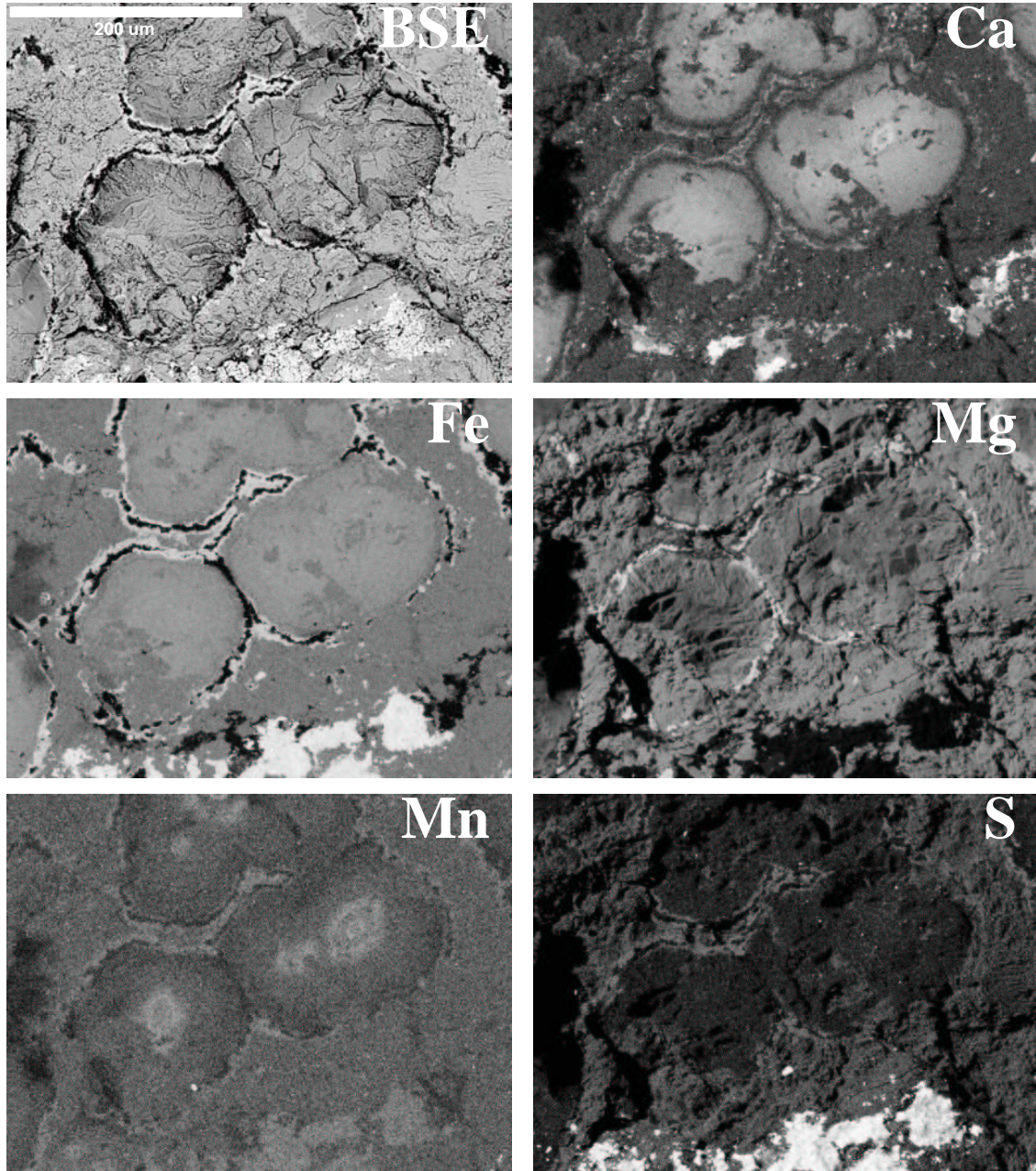


Figure 11: Backscattered electron and element maps of carbonate globule cluster F.

difference in this ratio between a globule with a radius of 50 μm and a globule with a radius of 100 μm does not produce a significant effect. (See figure 13).

Decreasing the amount of water in which a globule is immersed, on the other hand, does produce a significant effect. Immersed in 1 L of water, a globule will ultimately dissolve completely. In smaller volumes of water, dissolution is hampered by equilibrium effects. As Dresel (1989) noted, siderite dissolves to near equilibrium, stopping around a saturation index of -0.5. On the other hand, magnesite ceases dissolution when it reaches a saturation index of -1.7. This effect is clearly visible in the smaller water volume runs, as illustrated in figure 14.

Atmospheric composition also has a significant effect. While the modern terrestrial atmosphere produces an initial solution pH of 5.7, a 1 bar CO_2 atmosphere produces a pH of 3.9. This significantly increases the initial rate of both magnesite and siderite dissolution, as shown in the comparison of figures 14, 15, and 16. In the case of magnesite, while almost all magnesium surface sites are hydrated at both pH values, a lower pH promotes the formation of $>\text{CO}_3\text{H}$ sites over $>\text{CO}_3^-$ sites, thus increasing dissolution rate. In the case of siderite, the rate of dissolution far from equilibrium is almost entirely determined by H^+ activity. Over the course of a run, however, the pH of the solution can increase significantly; magnesite globules exposed to terrestrial carbon dioxide levels reached a steady state at pH levels around 9.3.

4 Discussion

The examination of the carbonate globules in ALH84001 reveals two types of zoning. The first kind, exhibited particularly in the Ca and Mn distributions of the globule, is possessed by each member of an overlapping set of globules. The second kind, exhibited in the Fe- and Mg-rich rims of the globules, is usually shared collectively by members of an overlapping set. This distinction suggests that two types of processes produced the zonation patterns. A primary growth process likely resulted in Ca and Mn zonation, while a secondary weathering process, either on Earth or in Antarctica, could have produced the rims. This finding agrees with Eiler et al. (2002)'s determina-

Magnesite and Siderite Comparative Dissolution Rates

100 μm globule in terrestrial (350 ppm CO_2) atmosphere

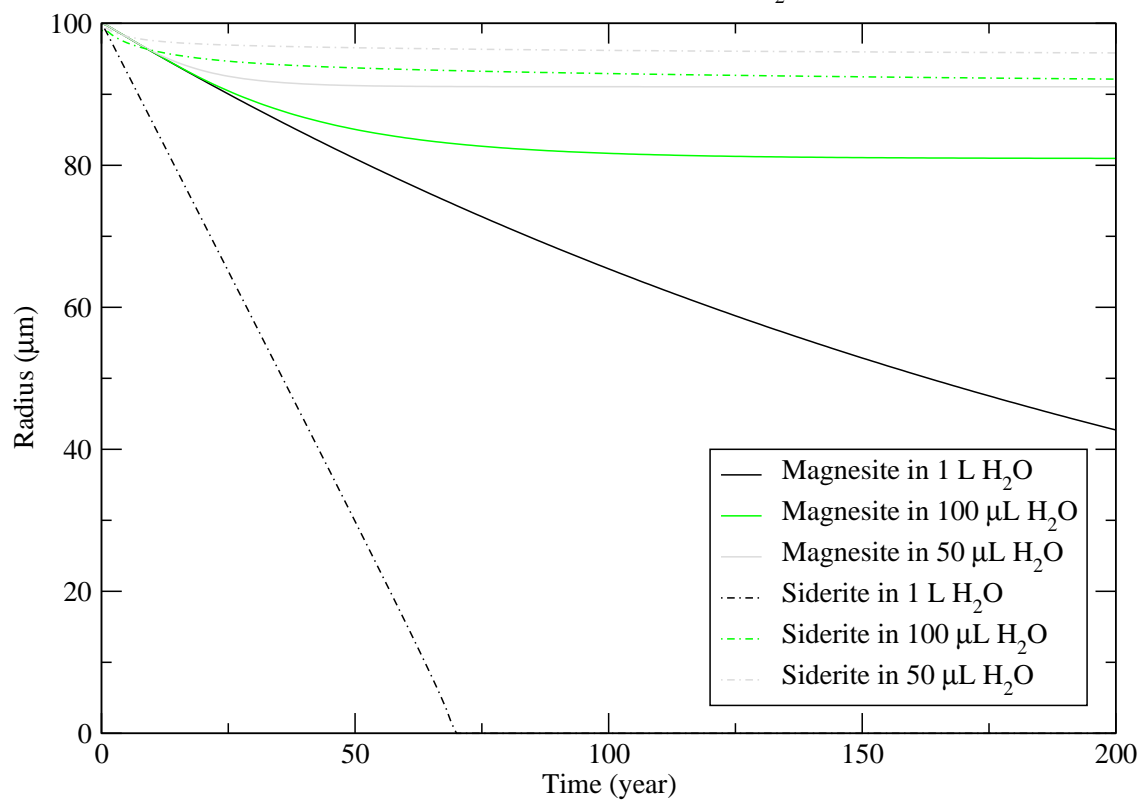


Figure 12: Comparative dissolution rates of 100 μm radius magnesite and siderite globules in varying amounts of liquid water.

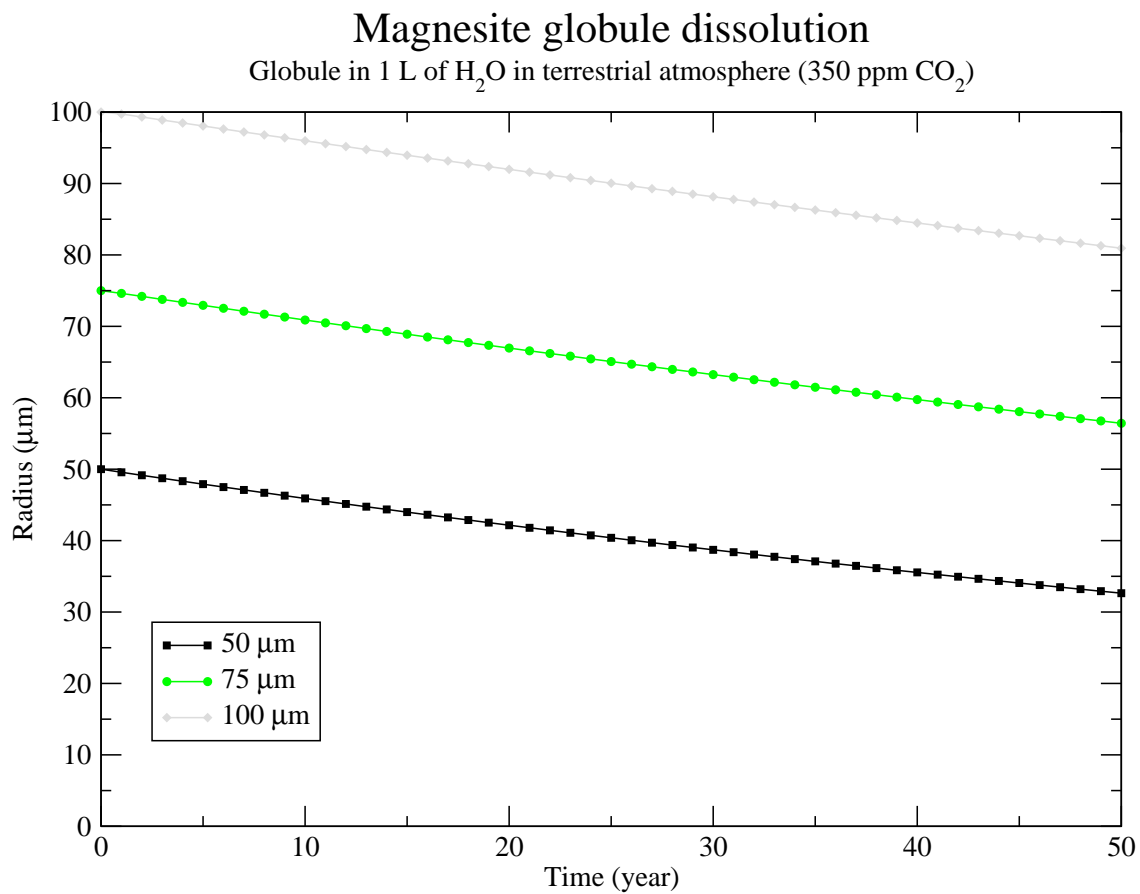


Figure 13: Comparative dissolution rates of magnesite globules of varying radii in 1 L of liquid water initially in equilibrium with an atmosphere of terrestrial composition, containing 350 ppm CO₂.

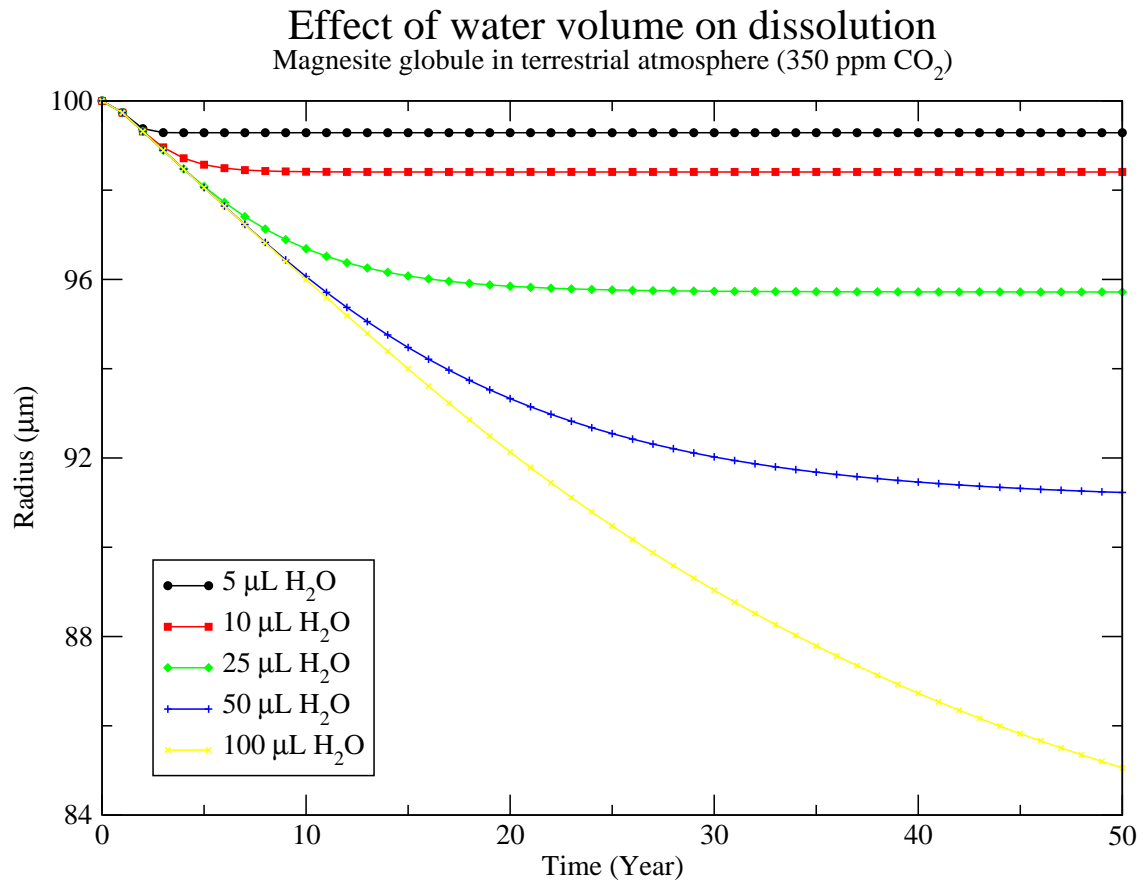


Figure 14: Comparative dissolution rates of 100 μm radius magnesite globules in varying amounts of liquid water initially in equilibrium with an atmosphere of terrestrial composition, containing 350 ppm CO₂.

Effect of water volume on dissolution Magnesite globule in Martian atmosphere (8 mbar CO₂)

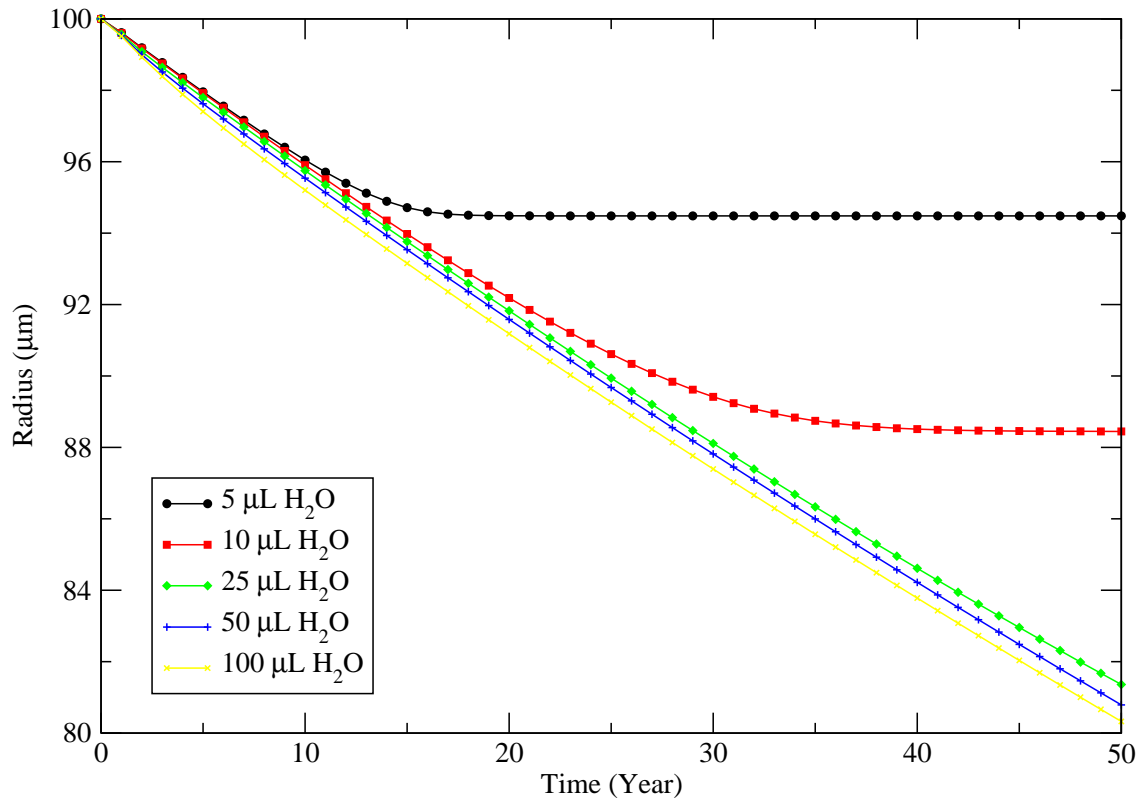


Figure 15: Comparative dissolution rates of 100 μm radius magnesite globules in varying amounts of liquid water initially in equilibrium with an atmosphere of modern Martian composition, containing 8 mbar CO₂.

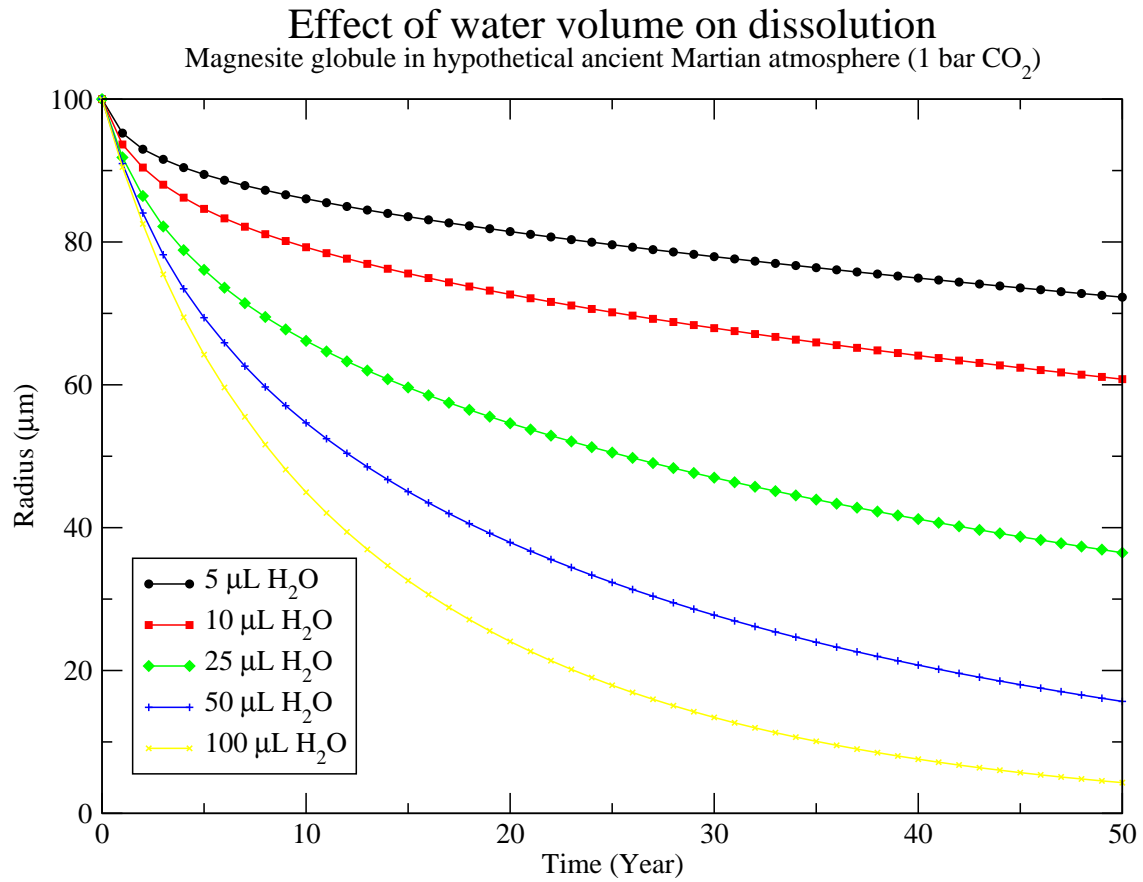


Figure 16: Comparative dissolution rates of 100 μm radius magnesite globules in varying amounts of liquid water initially in equilibrium with a thick 1 bar CO₂ atmosphere.

tion that the interiors of the globules consist of single crystals, while the rims are polycrystalline.

The interiors of the carbonate globules in ALH84001 are composed of magnesite, with significant amounts of FeCO_3 and CaCO_3 . Since calcite dissolves several orders of magnitude faster than magnesite or siderite, the MgCO_3 and FeCO_3 components of the globules will be the main regulators of their dissolution rate. Since magnesite and siderite dissolve at fairly similar rates, it is reasonable to assume that the iron-rich magnesite globules in ALH84001 will dissolve at about the same rate as pure phases of these minerals.

The results of the kinetic model therefore suggest that a carbonate disc, composed primarily of magnesite, exposed to a sufficient amount of water initially in equilibrium with the terrestrial atmosphere, could be reduced in radius by $10\ \mu\text{m}$ in under fifty years. A minimum of $50\ \mu\text{L}$ of water would be needed if this dissolution were to occur in a continuous period of time. If the carbonate were exposed to a larger volume of water, a $10\ \mu\text{m}$ reduction in radius would occur after about 25 years, but the carbonate would continue to dissolve. Smaller amounts of water would suffice if repeating cycles of wetness and dryness occurred. If such exposure had occurred not on Earth, but on an ancient Mars with a thick CO_2 atmosphere, the exposure must have been extremely brief for the entire globule not to dissolve.

ALH84001 was almost certainly exposed to Antarctic surface conditions before its discovery in 1984 for sufficient time to allow a $10\ \mu\text{m}$ radius annulus to dissolve. The Antarctic meteorite LEW 85320, a H5 chondrite, has been on the Earth for about 32 k.y., about two-and-a-half times longer than ALH84001. Nevertheless, carbon-14 analysis of nesquehonite [$\text{Mg}(\text{HCO}_3)(\text{OH})\cdot 2\text{H}_2\text{O}$] found on the surface of the meteorite revealed that this carbonate had been forming over the thirty years prior to the meteorite's recovery (Jull et al., 1988), which implies that it had been exposed to surface conditions favorable for carbonate formation for at least this amount of time.

During ALH84001's period at the surface, liquid water could have infiltrated the carbonate-containing fractures within it. When the water evaporated, fine-grained carbonate like that of the globule rims would have been left behind. If too large an amount of water entered the rims, however, the fine-grained carbonate would not be localized in the rims. In some instances, this is the case.

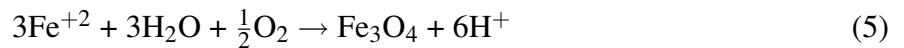
Species	ΔG_f° (kJ/mol)
H ₂ (g)	0
H ⁺	0
H ₂ O(l)	-237.13
O ₂ (g)	0
CO ₂ (g)	-394.36
Fe ⁺²	-85.35
Fe ⁺³	-11.05
Fe(OH) ₂	-486.2
FeO(OH) (goethite)	-488.7
Fe(OH) ₃ (amorphous)	-696.5
Fe ₂ O ₃ (hematite)	-742.2
Fe ₃ O ₄ (magnetite)	-1015.4
FeCO ₃ (siderite)	-666.67
H ₂ S	-27.83
SO ₄ ⁻²	-744.53

Source: Drever (1988).

Table 2: Standard Gibbs free energies of formation of species used in the construction of iron stability diagrams.

Wentworth et al. (1998) found blade-like to rhombohedral Mg-carbonate crystals near carbonate globules that they suggested were hydrated forms of Mg-carbonate.

Water entering a fracture during a period of wetness would have dissolved Mg⁺², Fe⁺², and CO₃⁻² ions (along with other trace components) from the carbonate. Fe⁺² ions would have reacted with any free oxygen molecules to produce magnetite in the reaction



The presence of magnetite, rather than other iron oxides, in the carbonate rims constrains oxygen fugacity during the period of precipitation. The iron stability diagram in figure 17, constructed using the Gibbs free energies listed in table 2, shows that magnetite precipitation occurs only when oxygen fugacity falls below 10⁻⁶⁷ bar. As illustrated in figure 18, magnetite is always more stable than siderite under terrestrial conditions.

As some of the water dissolving the globule evaporated, magnesite would have been precipi-

Iron species stability as function of pH and fO_2

$T = 298 \text{ K}$, $pCO_2 = 350 \text{ ppm}$, $a(Fe^{+2}) = 10^{-4} \text{ M}$

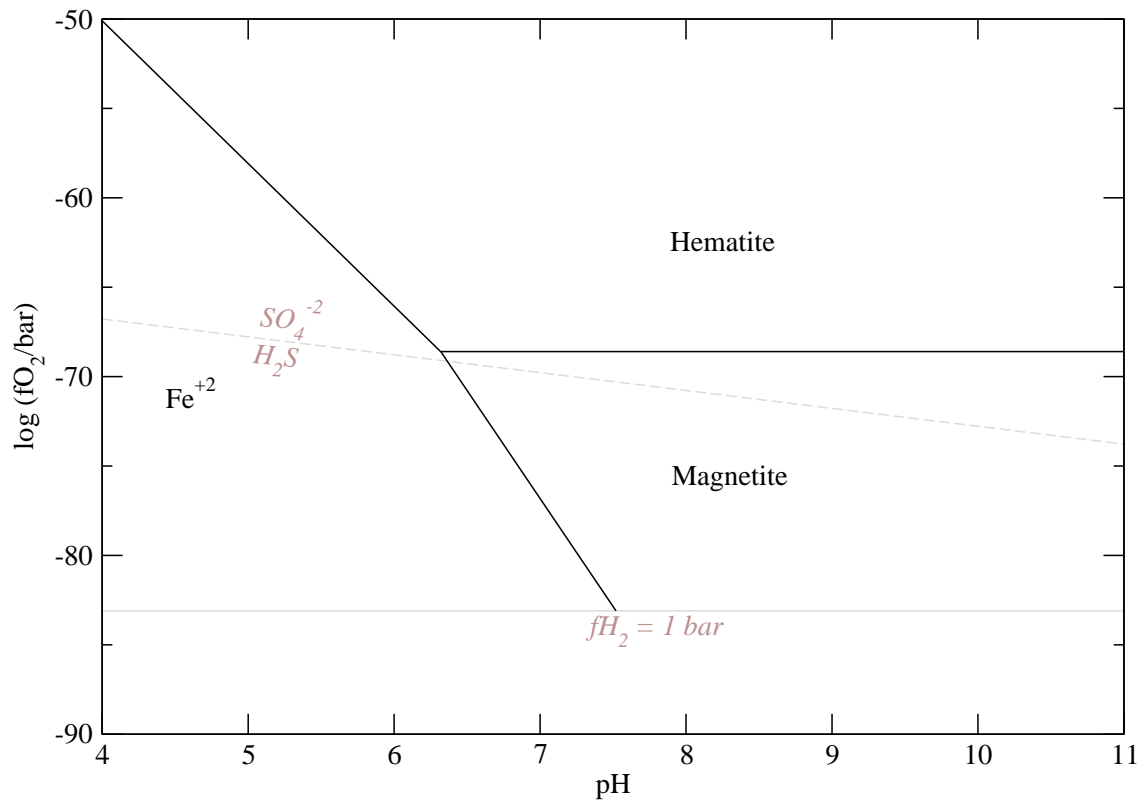


Figure 17: Stability relations of iron exposed to liquid water at 25°C, plotted as a function of pH and log oxygen fugacity.

Iron species stability as a function of $p\text{CO}_2$ and $f\text{O}_2$

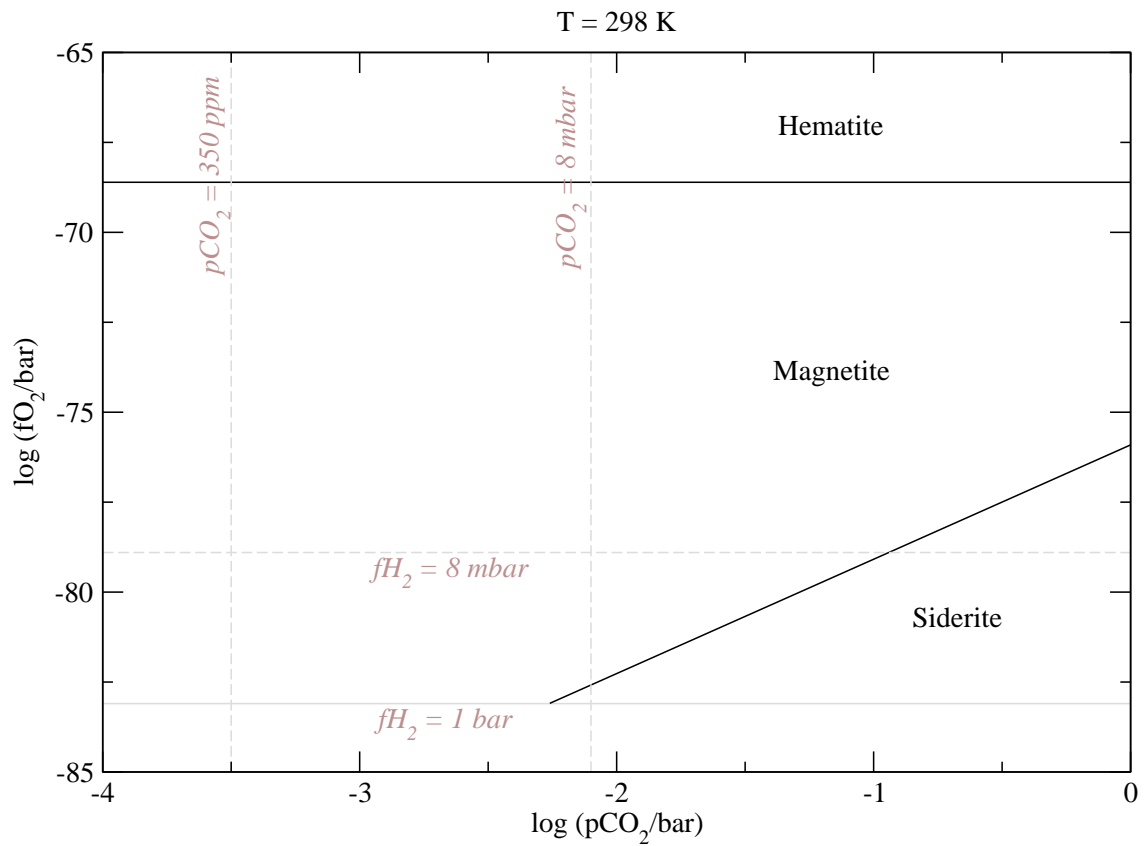
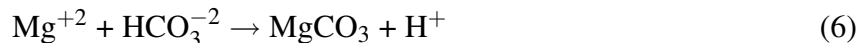


Figure 18: Stability relations of iron exposed to liquid water at 25°C, plotted as a function of CO_2 partial pressure and log oxygen fugacity.

	Globule D			Globule E		
	Interior	Rim	Bulk	Interior	Rim	Bulk
MgCO ₃	64.95%	62.64%	63.84%	61.07%	69.95%	65.24%
Fe(CO ₃ ,O _{1.33})	27.27%	31.85%	29.47%	30.61%	24.60%	27.61%
CaCO ₃	7.16%	4.48%	5.88%	7.78%	4.74%	6.57%
MnCO ₃	0.62%	1.02%	0.81%	0.54%	0.71%	0.58%

Table 3: Integrated compositions of ALH84001 carbonate globules based on X-ray analysis.

tated in the reaction



During a subsequent period of greater wetness, much of the freshly precipitated fine-grained magnesite would have dissolved, but some of the water would have percolated through to continue dissolving the central crystal. The attack on the central crystal could have been completely halted only if a less soluble substance, such as magnetite, were precipitated in a fashion that prevented water from contacting the carbonate.

The hypothesis of an Antarctic origin for the carbonate rims makes two predictions about the composition of the rims. Chemically, the integrated composition of the rims should be similar to that of the outer zone of the central globule. The measurements made on the globules with the x-ray analysis system show that, while the bulk compositions of the rims are not identical to those of the globules as a whole, they are close. (See table 3.)

Isotopically, in contrast, the carbonate rims should be distinct from the central carbonate grains, as the rims would have incorporated terrestrial carbon and oxygen. Jull et al. (1995) and Jull et al. (1997) found that acid etching of carbonates released CO₂ with $F_m(^{14}\text{C})$ values ranging from 0.027 to 1.00, where $F_m(^{14}\text{C})$ is defined as the ratio of the concentration of ¹⁴C in the sample to that of the terrestrial atmosphere in 1950. This would be expected from a mixture of Martian carbon from the central grains and terrestrial carbon from the rims. All the ¹⁴C in the central grains should be cosmogenic, produced by spallation while the meteorite was in transit from Mars to Earth. This process would have produced a level of ¹⁴C in the meteorite equal to 4.3% of the 1950 terrestrial atmospheric level; since the meteorite landed on Earth, this value would have decayed to $F_m(^{14}\text{C}) = 0.009$. $F_m(^{14}\text{C})$ values expected for terrestrial carbonate would range from about 0.20 for ¹⁴C

incorporated when the meteorite landed ~13,000 y.a. to as high as 1.8 from modern ^{14}C . (Hydrogen bomb testing in the 1950's and 1960's produced a large enrichment of ^{14}C in the atmosphere.) Unfortunately, the absolute concentration of ^{14}C is too low to allow for high-resolution ion probe measurements to locate the source of the terrestrial ^{14}C .

While few ion probe measurements have been made of the $\delta^{13}\text{C}$ values of the globule rims, the $\delta^{18}\text{O}$ ion probe measurements presented by Eiler et al. (2002) are compatible with but not indicative of a terrestrial origin for the rims. $\delta^{18}\text{O}_{\text{SMOW}}$ of the globule interiors range between about 0‰ to about 21‰, while those from the rims range from about 13‰ to about 28‰. These heavy rim values are similar to those reported for Antarctic carbonates in LEW 85320 (Grady et al., 1989).

4.1 Speculations on the origins of magnetites and sulfides

If the carbonate rims are, indeed, of terrestrial origin, it is reasonable to look for a terrestrial origin for the magnetites and sulfides in the rims. As noted above, magnetite is produced by the proposed rim formation process. It may also have been produced by Antarctic magnetotactic bacteria living in the solution that dissolved the rock; this could explain the resemblance, noted by Thomas-Keprta et al. (2000), of some of the magnetite crystals to those produced by the magnetotactic bacteria strain MV-1.

The small quantity of sulfide minerals present in the rims may have similarly been produced by organisms acting within the rock, possibly reducing sulfate from sea spray. While pyrites embedded within the orthopyroxene matrix of ALH84001 have been found to have $\delta^{34}\text{S}$ values from -0.6‰ to +7.3‰ (Greenwood et al., 1997, 2000), sulfide grains associated with the carbonates can obtain $\delta^{34}\text{S}$ values as low as -9.69‰ (Greenwood et al., 2000). Such low values, over 30‰ less than the mean modern seawater sulfate value of +21‰ (Schlesinger, 1991), could have resulted from bacterial sulfate reduction.

Furthermore, while some of the pyrites exhibit mass-independent fractionation of sulfur isotopes, the small number of carbonate-associated sulfide grains measured so far have not (Greenwood et al., 2000). Mass-independent sulfur isotope fractionation has been observed in terrestrial

samples older than about 2 Ga and is believed to be the result of photochemical processes that could not occur at significant rates once the Earth's ozone layer formed (Farquhar et al., 2000). Mass-independent fractionation therefore would not be expected if the rim sulfides formed from reduction of sea spray sulfate.

In order for magnetite to form in the reaction described in equation 5, the solution within ALH84001 most have experienced low oxygen fugacities; at 25°C, fO_2 of below 10^{-69} bar is required for magnetite, rather than hematite, to be the stable form of iron oxide. This is compatible with sulfate reduction having occurred in the meteorite, as the sulfate reduction reaction



would buffer oxygen fugacity and maintain it within the magnetite stability field.

The coexistence of potentially biogenic magnetite and potentially biogenic sulfides in the Fe-rich rims of the carbonate globules is also compatible with biological activity during the formation of these rims.

5 Conclusion

Among the strongest arguments by McKay et al. (1996) that ALH84001 bears evidence of former Martian life are their claims that the carbonate globules in the rock formed at temperatures compatible with the existence of life and that the magnetites and sulfides associated with the globules, located primarily in the globule rims, resemble those that might be produced by biological activity.

The petrographic observations described in this paper suggest that the carbonate globules formed through a two-stage process involving growth followed by partial dissolution and reprecipitation. The kinetic model described in this paper suggests that sufficient time was available while ALH84001 was on the surface in Antarctica for the globule rims to have been formed there by the dissolution of primary Martian carbonates and the precipitation of secondary magnesite and magnetite. If magnetite were formed in this process, it would require the oxygen fugacity of the

dissolving fluid to have passed through levels compatible with sulfate reduction, which could have produced the sulfides associated with the carbonate rims. If this model is correct, then any biogenic features in the carbonate globule rims are most probably indicative not of life on ancient Mars, but of life on modern Earth.

Looking for signs of ancient life in a Martian rock, randomly collected from its parent body and stripped of all context, would under the best of circumstances be a challenging task. It is unlikely that the question of whether life existed on ancient Mars can be solved without thorough field work by robotic and human explorers.

6 Acknowledgments

Many thanks to Munir Humayun for the support he has provided me over the past three years, and my family for the support they have provided me for the past 21 years. Thanks also to:

- Andy Campbell, for helping me make the SEM measurements described in this paper;
- The faculty, staff, and students of the Department of Geophysical Sciences;
- Carl Sagan and Isaac Asimov, for inspiration; and
- John D. Rockefeller, William Rainey Harper, Robert Maynard Hutchins, Edward Levi, and the other colorful characters who made the University of Chicago and the College what they are today.

References

- Becker, L., Glavin, D. P., Bada, J. L., 1997. Polycyclic aromatic hydrocarbons (PAHs) in Antarctic Martian meteorites, carbonaceous chondrites, and polar ice. *Geochimica et Cosmochimica Acta* 61, 475–481.
- Becker, L., Popp, B., Rust, T., Bada, J. L., 1999. The origin of organic matter in the Martian meteorite ALH84001. *Earth and Planetary Science Letters* 167, 71–79.
- Borkovec, M., Westall, J., 1983. Solution of the Poisson-Boltzmann equation for surface excesses of ions in the diffuse layer at the oxide-electrolyte interface. *Journal of Electroanalytical Chemistry* 150, 325–337.
- Bradley, J. P., Harvey, R. P., McSween, H. Y., 1997. No ‘nanofossils’ in Martian meteorite. *Nature* 390, 454–456.
- Clayton, R., 1993. Oxygen isotope analysis. In: Score, R., Lindstrom, M. (Eds.), *Antarctic Meteorite Newsletter* 16(3). Johnson Space Center, Houston, Texas, USA, p. 4.
- Dresel, P. E., 1989. The dissolution kinetics of siderite and its effect on acid mine drainage. Ph.D. thesis, Pennsylvania State University, 264 pp.
- Drever, J. I., 1988. *The Geochemistry of Natural Waters*, 2nd Edition. Prentice Hall, Englewood Cliffs, NJ, USA, 437 pp.
- Dzombak, D., Morel, F., 1990. *Surface complexation modeling: Hydrous ferric oxide*. John Wiley, New York, NY, USA, 393 pp.
- Eiler, J. M., Valley, J. W., Graham, C. M., Fournelle, J., 2002. Two populations of carbonate in ALH84001: geochemical evidence for discrimination and genesis. *Geochimica et Cosmochimica Acta* 66, 1285–1303.
- Farquhar, J., Bao, H., Thiemens, M., 2000. Atmospheric influence of Earth’s earliest sulfur cycle. *Science* 289, 756–758.

- Golden, D. C., Ming, D. W., Schwandt, C. S., Lauer, H. V., Socki, R. A., Morris, R. V., Lofgren, G. E., McKay, G. A., 2001. A simple inorganic process for formation of carbonates, magnetite, and sulfides in Martian meteorite ALH84001. *American Mineralogist* 86, 370–375.
- Golden, D. C., Ming, D. W., Schwandt, C. S., Morris, R. V., Yang, S. V., Lofgren, G. E., 2000. An experimental study on kinetically-driven precipitation of calcium-magnesium-iron carbonates from solution: Implications for the low-temperature formation of carbonates in Martian meteorite Allan Hills 84001. *Meteoritics and Planetary Science* 35, 457–465.
- Grady, M. M., E. K. Gibson, J., Wright, I. P., Pillinger, C. T., 1989. The formation of weathering products on the LEW 85320 ordinary chondrite: Evidence from carbon and oxygen stable isotope compositions and implications for carbonates in SNC meteorites. *Meteoritics* 24, 1–8.
- Grady, M. M., Wright, I. P., Pillinger, C. T., 1997. Microfossils from Mars: A question of faith? *Astronomy and Geophysics* 38, 26–29.
- Greenwood, J. P., Mojzsis, S. J., Coath, C. D., 2000. Sulfur isotopic compositions of individual sulfides in Martian meteorites ALH84001 and Nakhla: implications for crust-regolith exchange on Mars. *Earth and Planetary Science Letters* 184, 23–35.
- Greenwood, J. P., Riciputi, L. R., McSween, H. Y., 1997. Sulfide isotopic compositions in Shergottites and ALH84001, and possible implications for life on Mars. *Geochimica et Cosmochimica Acta* 61, 4449–4453.
- Harvey, R. P., McSween, H. Y., 1996. A possible high-temperature origin for the carbonates in the Martian meteorite ALH84001. *Nature* 382, 49–51.
- Jull, A., Cheng, S., Gooding, J., Velbel, M., 1988. Rapid growth of magnesium-carbonate weathering products in a stony meteorite from Antarctica. *Science* 242, 417–419.
- Jull, A. J. T., Courtney, C., Jeffrey, D. A., Beck, J. W., 1998. Isotopic evidence for a terrestrial source of organic compounds found in Martian meteorites Allan Hills 84001 and Elephant Moraine 79001. *Science* 279, 366–369.

- Jull, A. J. T., Eastoe, C. J., Cloudt, S., 1997. Isotopic composition of carbonates in the SNC meteorites, Allan Hills 84001 and Zagami. *Journal of Geophysical Research - Planets* 102, 1663–1669.
- Jull, A. J. T., Eastoe, C. J., Xue, S., Herzog, G. F., 1995. Isotopic composition of the carbonates in the SNC meteorites Allan Hills 84001 and Nakhla. *Meteoritics* 30, 311–318.
- McKay, D. S., E. K. Gibson, J., Thomas-Keptra, K. L., Vali, H., Romanek, C. S., Clemett, S. J., Chillier, X. D. F., Maechling, C. R., Zare, R. N., 1996. Search for past life on Mars: Possible relic biogenic activity in Martian meteorite ALH84001. *Science* 273, 924–930.
- McSween, H. Y., Harvey, R. P., 1998. An evaporation model for formation of carbonates in the ALH84001 Martian meteorite. *International Geology Review* 40, 774–783.
- Mittlefehldt, D. W., 1994. ALH84001, a cumulate orthopyroxenite member of the Martian meteorite clan. *Meteoritics* 29, 214–221.
- Mittlefehldt, D. W., 1997. Macroscopic description of Allan Hills 84001 and the relative timing of events in its history. *Meteoritics and Planetary Science* 32, A93–A93.
- Parkhurst, D., Appelo, C., 1999. User's guide to PHREEQC (Version 2)—a computer program for speciation, batch-reaction, one-dimensional transport, and inverse geochemical calculations. No. 99-4259 in *Water-Resources Investigations Reports*. U.S. Geological Survey, <ftp://brrcrftp.cr.usgs.gov/geochem/unix/phreeqc/manual.pdf>.
- Pokrovsky, O. S., Schott, J., 1999. Processes at the magnesium-bearing carbonates solution interface. II. Kinetics and mechanism of magnesite dissolution. *Geochimica et Cosmochimica Acta* 63, 881–897.
- Pokrovsky, O. S., Schott, J., Thomas, F., 1999. Processes at the magnesium-bearing carbonates solution interface. I. A surface speciation model for magnesite. *Geochimica et Cosmochimica Acta* 63, 863–880.

- Romanek, C., Thomas, K., E.K. Gibson, J., McKay, D., Socki, R., 1995. Petrogenesis of carbon and sulfur-bearing minerals in the Martian meteorite ALH84001 (abstract). Abstracts of the Lunar and Planetary Science Conference 26, 1183–1184.
- Schlesinger, W., 1991. Biogeochemistry: An analysis of global change. Academic Press, San Diego, CA, USA, 443 pp.
- Scott, E. R. D., 1999. Origin of carbonate-magnetite-sulfide assemblages in Martian meteorite ALH84001. *Journal of Geophysical Research - Planets* 104, 3803–3813.
- Thomas-Keprta, K. L., Bazylinski, D. A., Kirschvink, J. L., Clemett, S. J., McKay, D. S., Wentworth, S. J., Vali, H., Gibson, E. K., Romanek, C. S., 2000. Elongated prismatic magnetite crystals in ALH84001 carbonate globules: Potential Martian magnetofossils. *Geochimica et Cosmochimica Acta* 64, 4049–4081.
- Warren, P. H., 1998. Petrologic evidence for low-temperature, possibly flood evaporitic origin of carbonates in the ALH84001 meteorite. *Journal of Geophysical Research - Planets* 103, 16759–16773.
- Wentworth, S., Thomas-Keprta, K. L., Taunton, A., Velbel, M., McKay, D., 1998. Possible weathering features in ALH84001 (abstract). Abstracts of the Lunar and Planetary Science Conference 29, 1793.